Mechanistic insights into Sb(III) adsorption and oxidation on MnO_2 facets

Rohit Kumar[†§], Song Chai[†§], Ran Mao[‡§], Yanpeng Chen[†§], Hasan Ubaid Ullah[‡§], Jianbo Shi[†§*], Li Yan[†§*]

[†]State Key Laboratory of Environmental Chemistry and Ecotoxicology, Research Center for Eco-Environmental Sciences, Chinese Academy of Sciences, Beijing 100085, China

[‡]Key Laboratory of Drinking Water Science and Technology, Research Center for Eco-Environmental Sciences, Chinese Academy of Sciences, Beijing 100085, China

[§]University of Chinese Academy of Sciences, Beijing 100049, China

Tel: +86 15101509384

E-mail: liyan@rcees.ac.cn

1. Text S1. Synthesis of MnO_2 facets

Synthesis of δ-001: The synthesis of δ-001 with stacked nanosheets involved the addition of 0.45 g $KMnO_4$, 0.1 g urea, 1 mL HCl (37 wt%), and 0.15 g cetyltrimethylammonium bromide (CTAB) into 40 mL deionized (DI) water. The mixture was then heated at 100 ^oC for 24 hours in a hydrothermal reactor. The ultimate precipitate was rinsed, dehydrated at a temperature of 90 ^oC overnight, and subjected to calcination for a duration of 2 hours at a temperature of 300 ^oC in the presence of air. The product was designated as δ-001.[1]

Synthesis of α-310: α-310 was synthesized using a hydrothermal redox process involving $KMnO_4$ and $(NH_4)_2C_2O_4$. During a standard process, 3.16 g of $KMnO_4$ and 1.38 g of $(NH_4)_2C_2O_4 \cdot H_2O$ were dissolved in 70 mL of DI water using strong magnetic stirring. Subsequently, the solution mixture was moved to a Teflon-lined stainless-steel autoclave with a volume of 100 mL. The autoclave was subjected to heating in an electric oven and maintained at a temperature of 180 °C for a duration of 24 hours. Once the autoclave had naturally cooled to the ambient temperature, the precipitates were gathered through the process of centrifugation, subjected to multiple washes using DI water, and subsequently dried at a temperature of 105 °C.[2]

Synthesis of α-110: Two distinct hydrothermal reaction methods were utilized in Teflon-lined autoclaves to produce α-110 nanowires with varying exposed planes. The synthesis of rectangular α-110 was achieved using a hydrothermal technique.[3] $KMnO_4$ (Aldrich, 99.0%) and NH_4F (Aldrich, 99.99%) were employed to synthesize α-110 through neutral hydrothermal conditions. As part of a typical procedure, a solution was created by completely dissolving 0.15 g of $KMnO_4$ and 0.037 g of NH_4F in 40 mL of water that had been purified twice, using magnetic stirring to assist the process. The resultant solution exhibited transparency. The solution was put into a 50

mL autoclave equipped with a Teflon liner. The autoclave was hermetically sealed and kept at a temperature of 150 ^{o}C for a duration of 24 hours. Subsequently, it was allowed to cool down to the ambient temperature without any external intervention. The suspension was thereafter subjected to alternating centrifugation with doubly DI water and ethanol many times. The resulting brown precipitate was then dried in an oven at a temperature of 80 ^{o}C for a duration of 10 hours.

Text S2. **In situ flow cell ATR-FTIR study**

The Thermo-Nicolet iS50R FTIR spectrometer, fitted with a horizontal attenuated total reflectance (ATR) cell from PIKE Tech and a liquid-nitrogen-cooled mercury-cadmium-telluride (MCT) detector, was used to perform in situ flow cell ATR-FTIR observations. For a standard experiment, a 0.5 mL solution containing 4.0 g/L of the adsorbent was applied onto the ZnSe crystal and allowed to dry naturally at room temperature. In order to eliminate the loosely adhered particles and other contaminants on the surface of the coated film, a solution of NaCl with a concentration of 0.04 M and a pH of 7 was employed to cleanse the surface. The rinsing process was carried out at a rate of 0.5 mL per minute until there was no observable alteration in the IR spectra, which took approximately 2 hours. A background spectrum was obtained by measuring and recording the absorbance of the coated film and ZnSe crystal. Subsequently, a solution containing 50 mg/L of Sb(III) in a 0.04 M NaCl solution was introduced into the flow cell at a pH of 7. Spectra ranging from 4000 to 650 cm^{-1} were obtained at 15-minute intervals until adsorption reached equilibrium, which took approximately 4 hours. During the process of collecting spectra, all solutions were thoroughly purged with nitrogen gas in the absence of light.

The spectra were collected and analyzed using the Omnic 9.2 software (Thermo Fisher Scientific Inc., USA), which involved performing subtraction, normalizing, and baseline correction. The

spectra were deconvoluted using the PeakFit software package (Systat Software Inc). The number and centroid positions of contributing bands were determined by calculating second-derivative spectra. The experimental spectra were subsequently adjusted by maximizing the amplitudes and widths of the Gaussian functions. The width of each band remained consistent throughout the fitting process.[4]

Text S3. Calculation of surface undercoordinated Mn site density

To compare the abundance of reactive Mn sites across facets, we calculated the surface undercoordinated Mn site density using a coordination-based criterion. For each facet, the number of undercoordinated surface Mn sites $\left(N_{Mn}^{uc}\right)$ was counted and normalized by the in-plane surface area A of the slab unit cell to give:

$$\rho_{Mn}^{uc} = \frac{N_{Mn}^{uc}}{A}(Mn/nm^2)$$

where A is the in-plane area of the slab (computed from lattice parameters as $A = absin\gamma$ (Table S1).

2. Figures

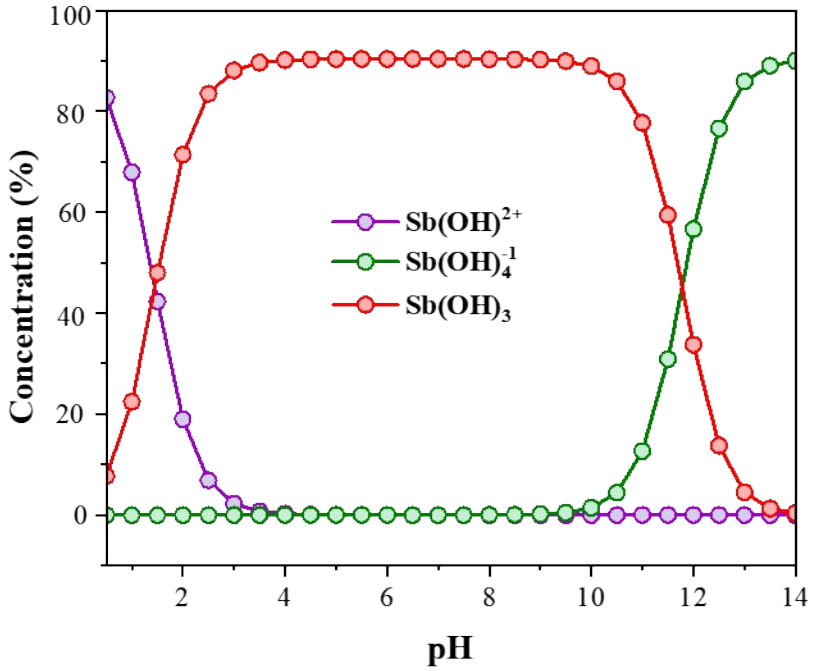

Fig. S1. The speciation of Sb(III) as a function of pH.

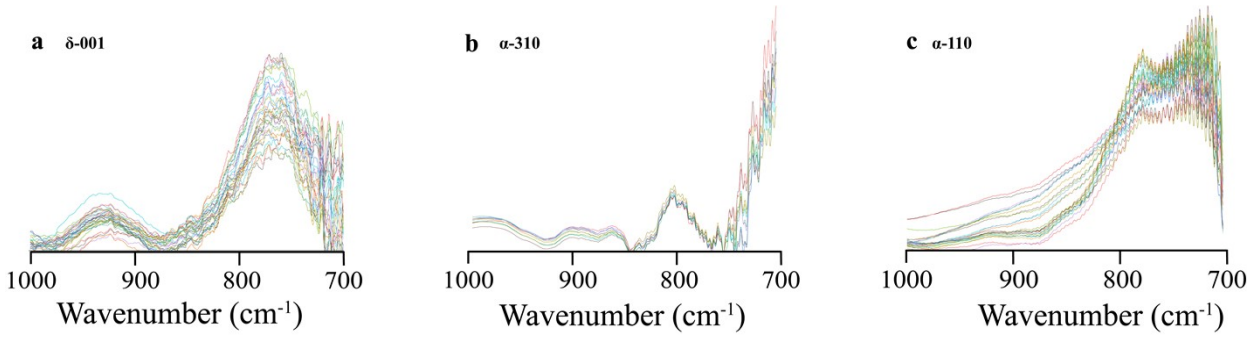

Fig. S2. (a-c) ATR-FTIR spectra of 50 mg/L Sb(III) adsorption on the δ-001, α-310, and α-110 MnO_2 facets with increasing time at pH 7. The samples were prepared by reacting 50 mg/L Sb(III) on 0.5 g/L MnO_2 in 0.04 M NaCl at pH 7.

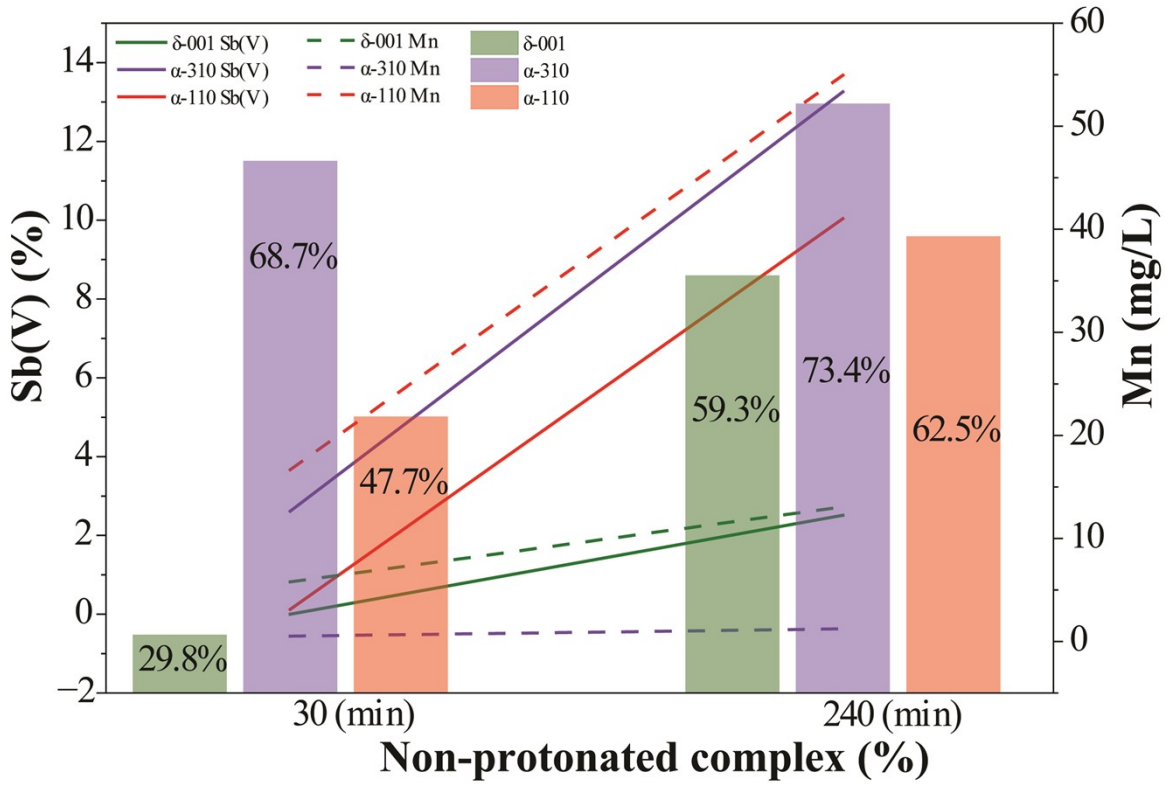

Fig. S3. The percentages of non-protonated Sb surface complex on δ-001, α-310, and α-110 MnO_2, and the relationship with Sb oxidation rate and Mn dissolution.

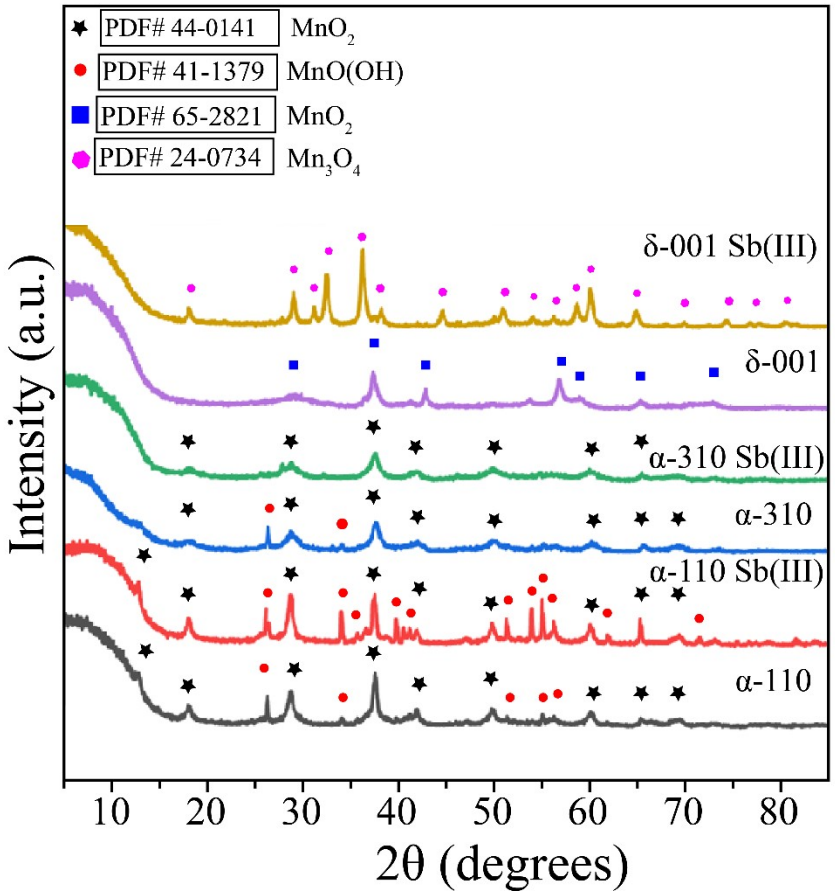

Fig. S4. XRD patterns for δ-001, α-310, and α-110 MnO_2 before and after Sb(III) adsorption.

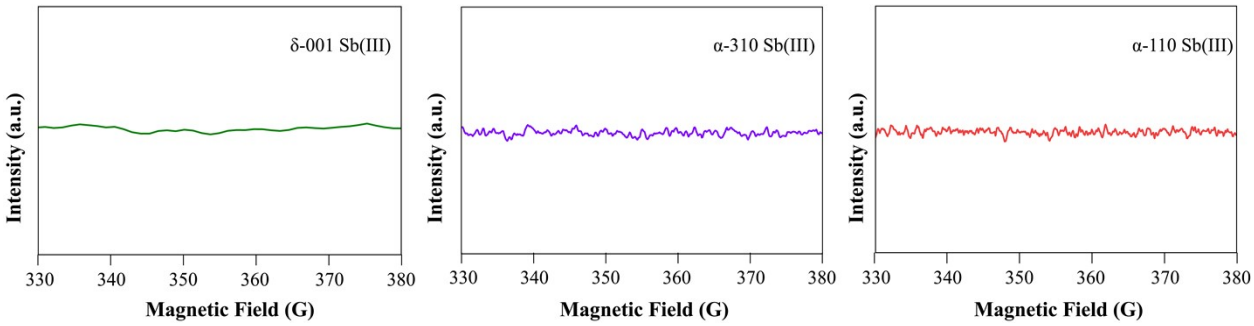

Fig. S5. EPR spectra of MnO_2 facets after Sb(III) adsorption in the presence of DMPO.

3. Tables

Table S1. Mn site density on different facets.

Facets	a(Å)	b(Å)	γ(°)	$A = \text{absin}\,\gamma$ (Å^2)	A (nm^2)	N_{Mn}^{uc}	$\rho_{Mn}^{uc} = \frac{N}{A}$ (Mn/nm^2)
δ-001	11.5935	11.3840	119.4041	114.98	1.1498	16	13.91
α -310	8.5410	15.5840	95.2409	132.55	1.3255	9	6.79
α-110	8.5410	14.1695	101.5911	118.55	1.1855	5	4.22

Table S2. Langmuir model parameters for Sb(III) adsorption on MnO_2 facets.

MnO_2 facets	Langmuir model		
	K (L/mg)	Qm (mg/g)	R^2
δ-001	0.00629	153.9	0.996
α -310	0.01824	107.3	0.981
α-110	0.11318	70.4	0.971

Table S3. Kinetic models parameters for Sb(III) adsorption on MnO_2 facets.

MnO_2 facets	pseudo-first-order model		pseudo-second-order model	
	k_1 (g·mg^{-1}·min^{-1})	R^2	k_2 (g·mg^{-1}·min^{-1})	R^2
δ-001	0.97717	0.969	0.00021	0.988
α -310	0.97937	0.965	0.00018	0.976
α-110	1.00001	0.972	0.00002	0.970

Table S4. Peak fit and calculated modes of IR spectra for 50 mg/L Sb(III) adsorption on MnO_2 facets.

Color in the given figure	Peak position (cm^{-1})	Peak area (%)	Assignments	Calculated position (cm^{-1})
δ-001 Sb(III) 30 min				
Blue	770	37.8	ν Mn-O = $(Mn-O)_2$-Sb(III)-OH	771
Olive	846	32.2	ν Sb(III)-O-Mn = $(Mn-O)_2$-Sb(III)-OH	830
Magenta	920	29.8	ν Mn-O = Mn-O-Sb(III)-O_2	913
δ-001 Sb(III) 240 min				
Blue	755	45.6	ν_s Sb(V)-O-Mn = $(Mn-O)_2$-Sb(V)-O_4	752
Olive	782	31.1	ν Mn-O = $(Mn-O)_2$-Sb(III)-OH	771
Magenta	825	9.4	ν Sb(III)-O-Mn = $(Mn-O)_2$-Sb(III)-OH	830
Yellow	923	13.7	ν Mn-O = Mn-O-Sb(III)-O_2	913
α-310 Sb(III) 30 min				
Blue	751	37.6	ν_s Sb(V)-O-Mn = $(Mn-O)_2$-Sb(V)-O_4	752
Olive	817	13.9	ν_s Sb(III)-O-Mn = $(Mn-O)_2$-Sb(III)-O	799
Magenta	852	11.8	ν Sb(III)-O-Mn = $(Mn-O)_2$-Sb(III)-OH	855
Yellow	922	17.2	ν Mn-O = Mn-O-Sb(III)-O_2	913
Sky	956	19.3	ν Mn-O = $(Mn-O)_2$-Sb(III)-OH	974
α-310 Sb(III) 240 min				
Blue	757	47.2	ν_s Sb(V)-O-Mn = $(Mn-O)_2$-Sb(V)-O_4	752
Olive	809	5.4	ν_s Sb(III)-O-Mn = $(Mn-O)_2$-Sb(III)-O	799
Magenta	855	4.3	ν Sb(III)-O-Mn = $(Mn-O)_2$-Sb(III)-OH	855
Yellow	919	20.8	ν Mn-O = Mn-O-Sb(III)-O_2	913
Sky	953	21.9	ν Mn-O = $(Mn-O)_2$-Sb(III)-OH	974
α-110 Sb(III) 30 min				
Blue	773	25.1	ν Mn-O = $(Mn-O)_2$-Sb(III)-OH	771
Olive	830	27	ν Sb(III)-O-Mn = $(Mn-O)_2$-Sb(III)-OH	830
Magenta	886	28.4	ν Mn-O = $(Mn-O)_2$-Sb(III)-O	878
Yellow	940	19.3	ν Mn-O = Mn-O-Sb(III)-O_2	913
α-110 Sb(III) 240 min				
Blue	733	40.2	ν Sb(V)-O-Mn = $(Mn-O)_2$-Sb(V)-O_4	735
Olive	773	37.3	ν Mn-O = $(Mn-O)_2$-Sb(III)-OH	771
Magenta	801	17.1	ν_s Sb(III)-O-Mn = $(Mn-O)_2$-Sb(III)-O	799
Yellow	925	5.2	ν Mn-O = Mn-O-Sb(III)-O_2	913

Table S5. XPS fitting results for pristine and Sb-adsorbed MnO_2 facets**.**

MnO_2 facets	δ-001 Pristine	δ-001 Adsorbed	α-310 Pristine	α-310 Adsorbed	α-110 Pristine	α-110 Adsorbed
Mn (III)	72%	65%	74%	74%	65%	51%
Mn(IV)	28%	35%	26%	26%	35%	49%
O_{ads}	35%	39%	52%	19%	42%	34%
O_{lat}	65%	24%	48%	20%	58%	26%
Sb(III)		32%		28%		32%
Sb(V)		5%		33%		8%

Table S6. XPS fitting results for Mn(III)/Mn(IV) and O_{ads}/O_{lat} ratios for pristine and Sb-adsorbed samples**.**

MnO_2 facets	Mn(III)/Mn(IV) Pristine	Mn(III)/Mn(IV) Adsorbed	O_{ads}/O_{lat} Pristine	O_{ads}/O_{lat} Adsorbed
δ-001	2.6	1.9	0.5	1.6
α-310	2.8	2.8	1.0	0.9
α-110	1.9	1.0	0.7	1.3

Table S7. The comparison of Sb adsorption capacities, Mn dissolution, XPS, XRD and EPR results for Sb reaction on MnO_2.

Sample	Adsorption capacity q_{max} (mg/g)	Mn dissolution (mg/L)	pH	XPS Mn(III) (eV)	XPS Mn(IV) (eV)	XRD	EPR	References
δ-001 MnO_2	153.9	13	7	641.4	643.0	mineral transformation	–	This work
α-310 MnO_2	107.3	2	7	641.8	643.9	No detectable change	–	This work
α-110 MnO_2	70.4	54	7	641.0	642.4	mineral transformation	–	This work
α-MnO_2	116.1	22	7	642.1	643.2	Peak shifts	–	[5]
γ-MnO_2	109.1	15	7	642.2	643.2	Peak shifts	–	[5]
δ-MnO_2	108.6	5	7	642.4	643.5	Peak shifts	–	[5]
δ-MnO_2	42.6	–	7	–	–	mineral transformation	Mn(II) signal	[6]
α-MnO_2	34.5	–	7	–	–	mineral transformation	Mn(II) signal	[6]
MO-2	111.7	–	6	641.6	643.0	–	–	[7]
α-110	–	–	–	–	643.6	–	–	[3]
δ-001	–	–	–	640.6	641.2	–	–	[1]

References:

1. X. Zheng, J. Cai, Y. Cao, L. Shen, Y. Zheng, F. Liu, S. Liang, Y. Xiao and L. Jiang, Construction of cross-linked δ-MnO_2 with ultrathin structure for the oxidation of H_2S: Structure-activity relationship and kinetics study, *Appl. Catal. B: Environ*, 2021, **297**, 120402.
2. S. Rong, P. Zhang, F. Liu and Y. Yang, Engineering crystal facet of α-MnO_2 nanowire for highly efficient catalytic oxidation of carcinogenic airborne formaldehyde, *ACS Catal*, 2018, **8**, 3435-3446.
3. W. Li, X. Cui, R. Zeng, G. Du, Z. Sun, R. Zheng, S. P. Ringer and S. X. Dou, Performance modulation of α-MnO_2 nanowires by crystal facet engineering, *Sci. Rep*, 2015, **5**, 8987.
4. Y. Brechbühl, I. Christl, E. J. Elzinga and R. Kretzschmar, Competitive sorption of carbonate and arsenic to hematite: Combined ATR-FTIR and batch experiments, *J Colloid Interface Sci*, 2012, **377**, 313-321.
5. J. Nie, Z. Yao, P. Shao, Y. Jing, L. Bai, D. Xing, G. Yi, D. Li, Y. Liu and L. Yang, Revisiting the adsorption of antimony on manganese dioxide: The overlooked dissolution of manganese, *Chem. Eng. J.*, 2022, **429**, 132468.
6. D. Wei, J. Liu, Z. Luo and X. Xie, Insight into the reactions of antimonite with manganese oxides: Synergistic effects of Mn (III) and oxygen vacancies, *Water Res.*, 2023, **232**, 119681.
7. J. Luo, C. Hu, X. Meng, J. Crittenden, J. Qu and P. Peng, Antimony Removal from Aqueous Solution Using Novel α-MnO2 Nanofibers: Equilibrium, Kinetic, and Density Functional Theory Studies, *ACS Sustain. Chem. Eng*, 2017, **5**, 2255-2264.